Available online at www.sciencedirect.com
ScienceDirect
Journal of Magnetism and Magnetic Materials 320 (2008) 210–216
Journal of magnetism and magnetic materials
www.elsevier.com/locate/jmmm

Using a genetic algorithm to study properties of minimum energy states and geometrical frustration in artificial "spin ice" systems

A. León*, J. Pozo

Facultad de Ingeniería, Universidad Diego Portales. Ejército 441, Santiago, Chile

Received 16 February 2007; received in revised form 27 April 2007
Available online 3 June 2007

Abstract

This article reports the results of a study on the base state of artificially frustrated "spin ice" systems. We have studied the states of minimum energy reported by experimental studies on nanoscale ferromagnetic islands and the protocols employed to reach those states. The main technique employed in this study is a genetic algorithm that has been contrasted with two Montecarlo methods. Nanoscale islands are modeled through dipolar moments placed on a plane, rectangular array. Studies include the correlation between nanoscale islands, statistics on vertex types formed in the array for the minimum energy state and intermediate states. The results suggest a failure in the protocols adopted to minimize energy in these systems. A study on the efficiency between the devised genetic algorithm and the Montecarlo methods used in the research is also included.

Keywords: Frustration; Spin ice; Genetic algorithm

1. Introduction

Frustration or competition between interactions is a common feature of many systems in condensed matter [1]. One of the most common frustrated systems is ordinary water ice, in which hydrogen ions follow the so-called "ice rules" [2]. These rules require that the four hydrogen atoms surrounding each oxygen atom should be placed in a tetrahedral coordination such that two are close to the central oxygen atom and the other two are far from that atom, as shown in Fig. 1a. In magnetic materials frustration appears when the system cannot minimize its total energy, minimizing the energy in each individual spin–spin interaction [3–5]. In a conventional "spin ice" system [6,7], magnetic ions form a lattice of joined tetrahedra. Spins in these ions point either inward or outward (Fig. 1b). The dipole interaction favors an in–out array of the moment configuration, but not all pairs can be simultaneously satisfied. As a result, the system is frustrated.

At low temperatures, the spins in these materials freeze into exotic disordered states that have many of the features of spin glasses [8,9], but these ice-like states are different from disorder-based spin glasses in that there is a very narrow relaxation time of spins due to the well-ordered lattices [10,11].

One of the most fascinating aspects of magnetically frustrated systems is how they locally accommodate the spin–spin frustration. However, from a practical point of view, individual spins within the materials are difficult to be experimentally probed without altering the state of the system. To overcome this difficulty, magnetically frustrated systems have been created in which one can directly probe the individual elements without altering the state of the system. Previous works have been reported in which interacting moments are trapped by magnetic fields at low temperatures [12,13]. Other experimental works report analogies closer to conventional "spin ice" systems, using individual arrays of single-domain ferromagnetic systems [14–19]. In an excellent work by Wang et al. [20], they report a study on minimum energy states in a system formed by 80,000 nanoscale ferromagnetic islands on an array fabricated with lithographic techniques and with

*Corresponding author.
E-mail address: alejandro.leon@udp.cl (A. León).

0304-8853/$ - see front matter © 2007 Elsevier B.V. All rights reserved.
doi:10.1016/j.jmmm.2007.05.029

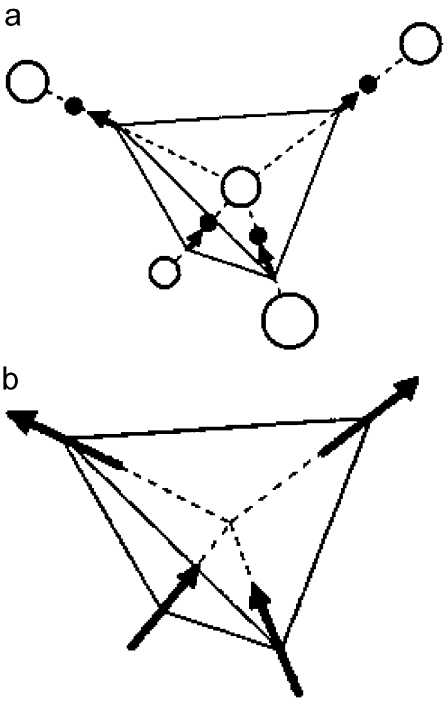

Fig. 1. (a) Schema of water ice with two hydrogen atoms far from the oxygen atom and two close to the atom. (b) "Spin ice" schema of a tetrahedrical lattice in a rare earth.

different lattice parameters. In the same issue of Nature, Bramwell [21] discusses the possible true states of minimum energy for those systems and the efficiency of the experimental protocol used to reach those states.

Here we report an study of the topological properties of nanoscale ferromagnetic islands in minimum energy states. We simulate the arrays studied in the experimental work by Wang et al., calculating the effective dipolar interaction between the particles. The techniques used to reach the minimum energy states are a genetic algorithm and two Montecarlo methods, which enable us to compare both methods.

2. Model and simulation

The system under study is composed of a two-dimension array of single-domain ferromagnetic islands with intrinsic moments. In order to make the comparison with the experimental work by Wang, we will use nanoscale islands of 80 nm width, 220 nm length and 25 nm height. The size is small enough to allow spins to be aligned in a single ferromagnetic domain, but large enough to allow stability of the configuration at 300 K. Interaction energy is in the order of 10^{-19} J, equivalent to 10^4 K. The moment of each island is in the order of 10^7 Bohr magnetotes. The smallest lattice parameter is on the range of 320 nm and it will be moved on to 900 nm. Part of the configuration of the array on the plane is represented in Fig. 2a. In our simulation we will study 1024 nanoscale islands which form a square array.

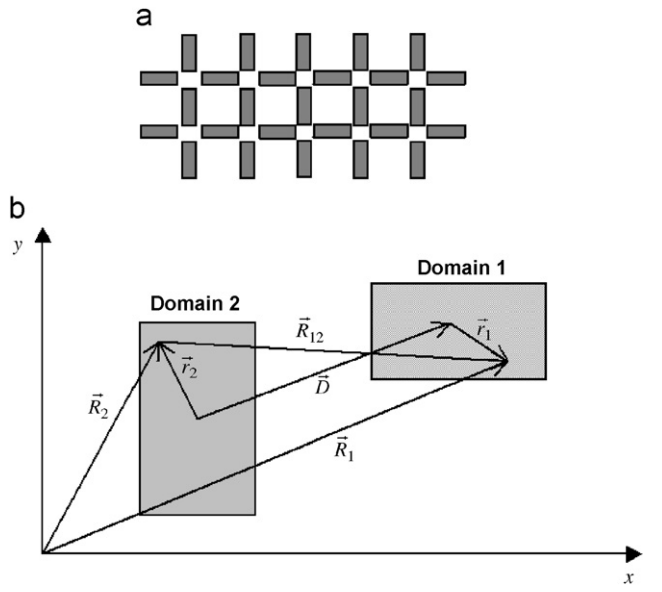

Fig. 2. (a) Array of nanoscale islands in a two-dimension square lattice. (b) Two interacting generic domains. Each spin within the domain placed in $\vec{R}_1$ interacts with each spin placed in $\vec{R}_2$ of domain 2.

In order to determine interaction energy between any domains in the array, we evaluate the effective dipolar interaction among these domains.

2.1. Effective dipolar interaction

We take two generic domains within the array and calculate the dipolar interaction between the spins of both particles, given by the following equation:

$$E_{\mathrm{dip}} = \frac{1}{2}\Omega\frac{t_1 t_2}{c_0^2} \times \sum_{\vec{R}_1\vec{R}_2}\left[\frac{\vec{s}_1\cdot\vec{s}_2}{R_{12}^3} - 3\frac{\vec{s}_1\cdot\vec{R}_{12}\,\vec{s}_2\cdot\vec{R}_{12}}{R_{12}^5}\right], \quad (1)$$

where $\Omega = g^2\mu_{\mathrm{B}}^2$ (g is the gyromagnetic factor and μ_{B} the Bohr magneton), c_0 is the interplane distance in the z direction, t_1 and t_2 represent the thickness of the nanoscale islands (in this case $t \ll L$ where L is the magnitude of the length of the nanoscale islands in the plane). As shown in Fig. 2b $\vec{D}$ represents the position vector of the mass center in one of the two domains respect to the mass center in the other domain. The energy of Eq. (1) can be expanded to the r/D ratio, in which r is the module of vector $\vec{r} = \vec{r}_2 - \vec{r}_1$. This expansion is documented in great detail in a work by Politi and Pini [22]. The equation for dipolar energy can be written as follows:

$$E \approx E_{\mathrm{dip}}^{(0)} + E_{\mathrm{dip}}^{(2)}, \quad (2)$$

where $E_{\mathrm{dip}}^{(0)}$ is the zero order coupling and $E_{\mathrm{dip}}^{(2)}$ takes into account the finite size of the nanoscale islands. These terms

are given by the following expressions:

$$E_{\mathrm{dip}}^{(0)} = \frac{\Omega}{2}\left[\frac{\vec{S}_1 \cdot \vec{S}_2}{D} - 3\frac{\vec{S}_1 \cdot \vec{D}\,\vec{S}_2 \cdot \vec{D}}{D^5}\right], \tag{3}$$

$$E_{\mathrm{dip}}^{(2)} = \Omega\frac{9\Gamma_{12}}{4}\frac{\vec{S}_1^{\perp} \cdot \vec{S}_2^{\perp}}{D^5} + \Omega\frac{3\Gamma_{12}}{4} \times \left[\frac{\vec{S}_1^{\parallel} \cdot \vec{S}_2^{\parallel}}{D^5} - 5\frac{\vec{S}_1^{\parallel} \cdot \vec{D}\,\vec{S}_2^{\parallel} \cdot \vec{D}}{D^7}\right]. \tag{4}$$

Each particle behaves as a $\vec{S} = N\vec{s}$ simple spin, where N is the total number of spins. In these expressions, $\vec{S}^{\parallel}$ and $\vec{S}^{\perp}$ represent, respectively, the spin components in the plane and perpendicular to the plane, Γ_{12} is the semi-sum of the inertia moments of the particles. In the present work we study the effects of the term $E_{\mathrm{dip}}^{(2)}$ on the lattice parameter.

2.2. Genetic algorithm

In order to obtain the configuration of moments with minimum energy, a genetic algorithm that searches in the space of the configurations will be used according to the following methodology:

- The possible configuration of moments (simple spins) will be represented by individuals having a specific genotype. The genes represent the position of the nanoscale islands and the magnetic moment. These genes determine the phenotype of each individual in a population, the energy of the system, the type of vertex, the correlation, etc.
- Hundred individuals are randomly chosen, and the total energy of the system for each individual is determined. The quality of each individual for adaptation is determined by its energy. The lower the energy the better the quality.
- A diversity mark is given to individuals. They are ordered in a more or less diverse order according to different descriptors (gene diversity, vertex diversity, etc.)
- A survival probability is assigned to individuals ordered according to their quality and diversity, assigning 100% survival probability to the individual with less energy.
- Mutation operators and gene recombination are applied to surviving individuals in order to obtain the newer generation.

Due to the very high degeneration of states in this system, we have performed a search so as not to be trapped into a local minimum. This is achieved by means of diversity, which is far more important than the quality in this system. In every generation we have 100 individuals. The one showing the lower energy is chosen and the diversity of the remaining 99 individuals is calculated (e.g. referring to the vertex) respect to that chosen individual. When the second individual is chosen, diversity is measured respect to the two chosen individuals and so on, until 30 individuals are chosen. With those 30 individuals, 99 new elements are generated through mutations and recombinations. The lowest energy individual is added to this compound of 99 individuals and thus the new generation is obtained. The following table shows a part of this sequence and the way to choose individuals in each generation using the range space, that is, assigning a fix p probability of survival once the former individuals is chosen. In our case, the value of the probability is 40% once the individual with the lowest energy has been chosen (Table 1).

The advantage of this algorithm is the capacity to tunnel the barriers which separate the consecutive minimals when searching for possible solutions, using gene recombination. This procedure makes it possible to drastically reduce the dimension of the configuration space. Previous articles have reported the use of this technique in similar systems. For example, to study minimum energy states in 2- and 3-dimension spin glass [27].

In recent articles by Schmitt et al. [25,26], they showed the asymptotic convergence of genetic algorithms scaled to a global optima. If our algorithm is represented by a Markov Chain, it is possible to verify its compliance with the properties of the family of genetic algorithms that converge in a global optima. These properties are: alphabet (0, 1), multiple-bit mutation, single-cut-point crossover and power-law scaled proportional fitness selection based upon a fitness function. In the same article by Schmitt [25,26], they show both strong and weak ergodicity for these algorithms.

2.3. Montecarlo algorithm

We use a Montecarlo algorithm to work with "spin ice" systems in the lattice, as previously discussed in the works by Barkema and Newmann [23,24]. In this model, the "spin ice" configuration is mapped in the lattice using 3-color squares. In our work, we generalize this model to study any vertex configuration—not only spin ice configurations—using a 3-color code which does not necessarily comply with the rules of the model used by Barkema et al., as shown in Fig. 3a. The generalization means that in, in the

Table 1
Sequence to choose the second individual once the remaining 99 individuals have been ordered by combined range

Individual	Quality (Q)	Diversity (D)	Combined range $CR = 0.1Q + 0.9D$	Survival probability
I_{34}	58	3	8.5	0.400
I_{78}	67	5	11.2	0.240
I_{99}	99	2	11.7	0.144
I_{11}	50	10	14.0	0.086

The chart only shows the first four individuals.

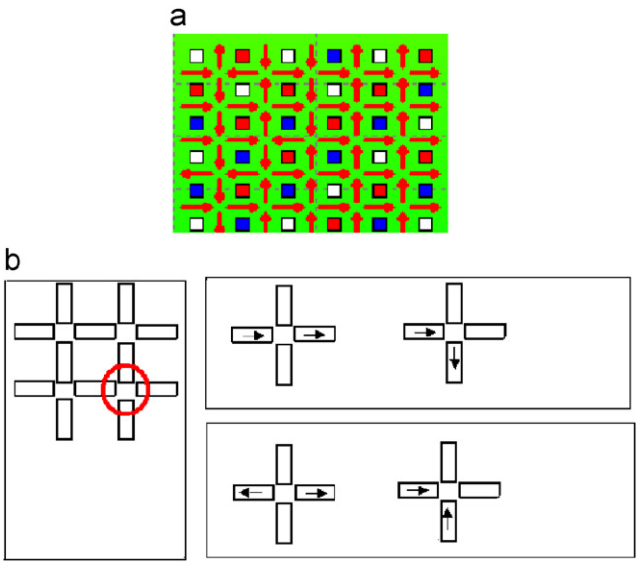

Fig. 3. (a) Configuration of "spin ice" (two in-two out) using a 3-code color in a section of the studied matrix. (b) Representation of vertex types studied in the array. (c) Vertex of the lattice with interacting pairs which favor minimization of energy (above) and vertex with energetically unfavorable pairs (below).

case of our algorithm, two consecutive squares can have the same color.

The methodology for using the Montecarlo method is the following:

- A configuration of random moments is implemented using a 3-color mapping for the squares which form the lattice studied (Fig. 3a), and its total energy is measured.
- A square is randomly chosen as the initial seed (be A the color of the square).
- From the two remaining colors, one is randomly chosen (color B), and a cluster is established. The cluster starts at the initial seed with the first neighbors of that seed and the nearest neighbors to those neighbors.
- A and B colors are interchanged in the cluster.
- The energy of the new configuration is measured and the change is accepted with the following probability.

$$P = \begin{cases} e^{-\beta \Delta E} & \text{if } \Delta E > 0, \\ 1 & \text{in another case.} \end{cases} \quad (5)$$

3. Results

In order to present the results of our simulation, we discuss the possible types of vertex configuration present in the array and the definition of the correlation between the nanoparticles. With this objective in mind, we reproduce the figures appearing in the work by Wang [20] in order to define the correlation. Fig. 3b shows the vertex defined by the four domains which form it. Fig. 3c shows the interaction of pairs in vertex types which favor or unfavor

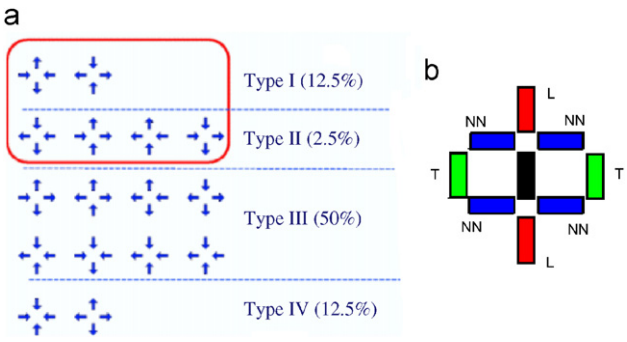

Fig. 4. (a) The 16 possible vertex types ordered from lower to higher energy and their percentage in a random initial configuration. (b) Definition of first neighbors in the correlation study.

minimization of energy. Fig. 4a shows the 16 possible vertex configurations of four nanoscale islands, separated into four topological types. These configurations are ordered from lower to higher energy. We can see that type I and II configurations correspond to "spin ice" vertex. As there are 16 possible configurations, we can determine the expected percentage of vertex types in a random distribution within the array.

In order to study the correlation between nanoscale islands, we will use the correlation function defined in the work by Wang et al. [20]. A set of correlation functions between different types of neighboring pairs is defined. "NN" represents the first neighbors in a nanoscale islands: "L" represents the next neighbors along the longitudinal direction to the nanoscale island, and "T" represents the next neighbors along the transverse direction. This configuration is shown in Fig. 4b. If the configuration of the pair is such that the energy of the dipolar interaction is minimized, then the correlation function takes the $C = +1$ value. If the configuration maximizes energy, then we get $C = -1$. Then we determine the average value of function C for NN, L and T pairs.

In our first simulation we just consider the effective dipolar interaction among all nanoscale islands within the array. Our array is composed of 1024 nanoscale islands distributed as shown in Fig. 2a. Using the genetic algorithm and the Montecarlo simulation we find the same minimum energy state with degeneration 2, which corresponds to the state proposed by Bramwell [21]. The configuration of moments in this state of minimum energy is represented in Fig. 5. In this configuration, 100% of vertexes is of Type I, and the average correlation for NN type pairs is $+1$. For T pairs, the average value of the correlation function is $+1$ and -1 for L pairs. These values imply that there is a strong correlation with the first neighbors in this state of configuration of moments. This configuration for the minimum energy is the same for all simulated lattice parameters.

Fig. 6a shows the energy of the base state when we include $E_{\mathrm{dip}}^{(2)}$ and when we do not consider it as a function of the lattice parameter. Using the information in the figure

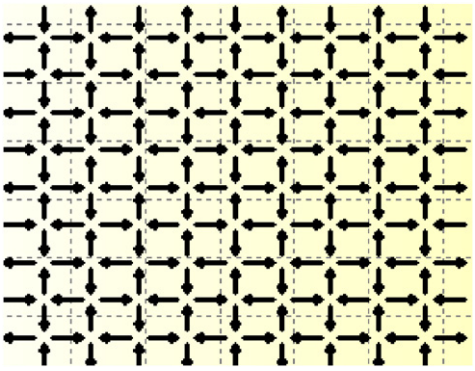

Fig. 5. Configuration of moments in the minimum energy state when considering only the effective dipolar interaction.

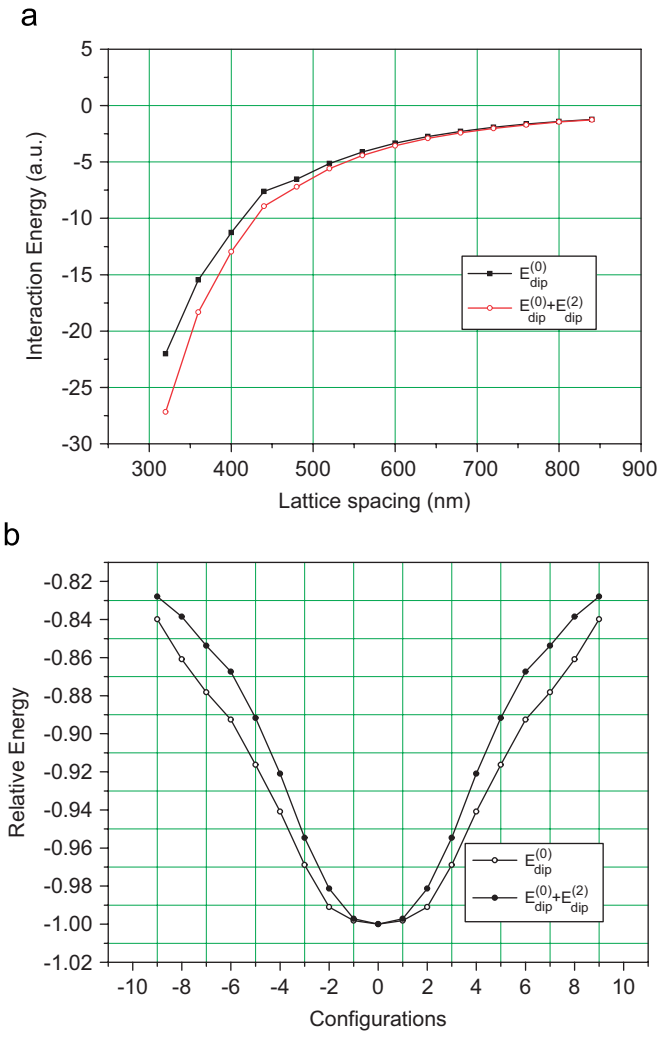

Fig. 6. (a) Study of the effect generated when considering the term in the effective bipolar energy of the array, as a function of the lattice parameter. The graph shows that the term that accounts for the shape of nanoscale islands is important in a spacing measuring less than 600 nm, supplying 19% of the total energy of the system, when the lattice spacing is 320 nm. (b) Comparison of energy (relative to the base state) for the first nine configurations of lower energy, when multipolar contribution is considered and when it is depreciated. The lattice parameter is 320 nm. A reflection is made in the y-axis for a better appreciation of the results. 0 configuration corresponds to the minimum energy state.

we can see that over 600 nm the effect of the form of nanoscale islands is irrelevant. In addition, when considering multipolar expansion, we include a study of the stability of the base state and of the first excited states, studying the first nine configurations of minimum energy in a fixed lattice parameter. In Fig. 6b, we show the energy of the system (relative to the minimum energy state) in two situations: one, when we consider the multipolar expansion which accounts for the shape and size of the nanoscale islands; two, when that term is depreciated. In the figure below we can see that the multipolar contribution helps to slightly stabilize the first two states of minimum energy.

3.1. Experimental protocol

In order to simulate the experimental protocol used in [20], we proceed as follows:

(1) In order to invert the magnetic moment of each nanoscale island, an $e>0$ energy should be delivered.
(2) First, a random configuration family is used, and in the expression which represents the energy of the system, the external magnetic field is incorporated.

$$E_i = E_{\text{dip}} - \vec{m}_i \cdot \vec{B} + \delta(\vec{m}_i - \vec{m}_0)e,$$

$$\text{where } \vec{B} = B_0(\cos(\omega t)\hat{i} + \sin(\omega t)\hat{j}), \tag{6}$$

δ is a function with value 1 when the moment $\vec{m}_i$ (at the n iteration of the genetic algorithm or Montecarlo algorithm), is equal at the initial moment for the same nanoscale island and zero in another case.
The algorithm preserves the configuration of $\vec{m}_i$ moments of the best individual in each iteration. The direction of the magnetic field rotates at velocity so as to simulate the effect of the rotation of the sample in the field. Time takes discreet values (corresponding to the iterations of the genetic or Montecarlo algorithm). The value of B_0 starts over the value of e and decreases in discreet steps (frequency v) until it reaches a value below e. The schema of the protocol used by the authors is shown in Fig. 7:

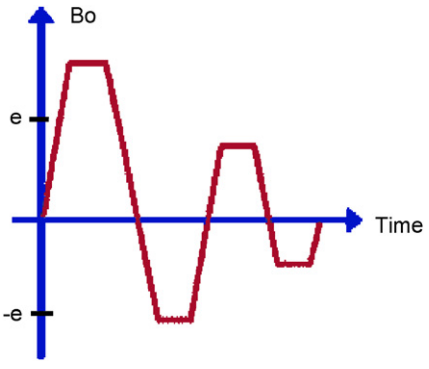

Fig. 7. Magnetic field applied to the sample in order to randomize moments in the nanoscales.

(3) The study includes the effect of achieving the minimum energy state for different values of angular velocity, as well as the frequency of changes in the direction and initial value of the field respect to the parameter.

The results are shown in Figs. 8 and 9. These results are obtained after determining the set of values (ω, v, B_0) which optimize the protocol to minimize energy. Figs. 8 and 9 show a study on types I and II vertexes (spin ice vertex) and NN type correlation. The study allows us to verify that with the method of the sample which rotates in the magnetic field, the system is unable to accommodate all configurations to minimize energy. This situation can be seen in greater detail if we study one rotating vertex and we verify the way in which the system adjusts itself, using its four moments, to minimize energy, and so the system is frustrated.

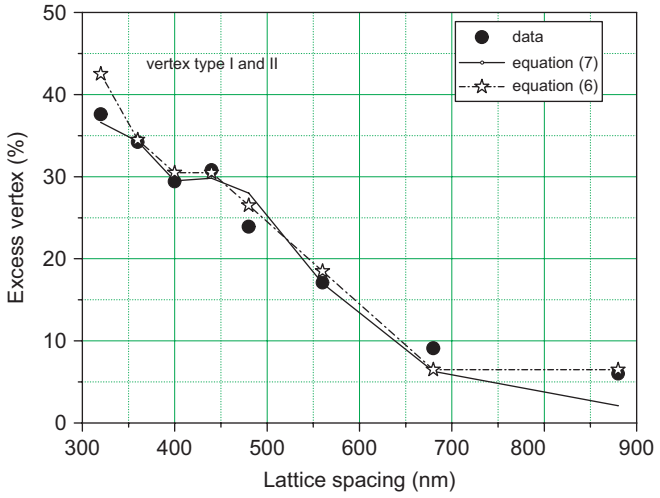

Fig. 8. Percentage of vertex excess as a function of lattice spacing for simulation and experimental data.

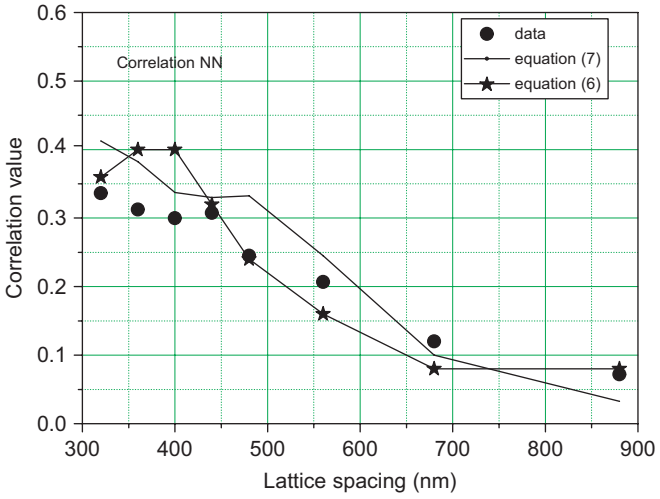

Fig. 9. Correlation between pairs of nanoscale islands as a function of lattice spacing for simulated and experimental data.

Similar results are obtained if we replace the experimental protocol simulation with another simulation of numeric origin.

We assume that it is difficult to reach the minimum energy state in the experimental protocol. To this aim, we calculate the energy of the system adding the following stochastic term to the dipolar interaction:

$$E_{\text{Total}} = \sum_{ij} [E^{(0)}_{\text{dip}} + E^{(2)}_{\text{dip}}]_{ij} + \alpha R P \delta(\vec{m}_i - \vec{m}_0), \tag{7}$$

where R is the total energy (as an absolute value) in the minimum energy state, P is a weight function with integer values ranging from 0 to 10, α is an adimensional parameter for adjustment. At the beginning of the simulation a $\vec{m}_0$ moment is assigned randomly to each nanoscale island and the value of the P function for each domain. With this additional term we can evaluate the energy that has to be used to flip the moments of the nanoscale islands, as a result of the inefficiency of the protocol.

4. Conclusions

The system studied shows a minimum energy state with degeneration two, and the configuration of moments is shown in Fig. 5. The minimum energy state is reached when considering only the effective, long-range dipolar interaction, using the three techniques described above, namely, the genetic algorithm, the Montecarlo method for "spin ice", and the general Montecarlo method. When we simulate the experimental protocol using a wide range of values for (ω, v, B_0), we cannot make the system achieve the minimum energy that can be achieved when only the effective dipolar interaction is considered. Using the best set of values for (ω, v, B_0), we can reproduce the experimental results reported in Ref. [20]. The same results can be achieved using Eq. (7). This methodology allowed us to assess the efficiency of the numerical techniques used to study this type of systems. We conclude that the 3-color Montecarlo method is more efficient when searching is done only in the space of "spin ice" configurations (type I and II vertices), but the genetic algorithm is far more efficient when searching starts at general configurations, that is, the four types of vertices. This is vitally important when studying the protocol with Eqs. (6) or (7).

References

[1] G. Toulouse, Commun. Phys. 2 (1977) 115.
[2] L. Pauling, The Nature of the Chemical Bond 301–304, Cornell Univ. Press, Ithaca, New York, 1945.
[3] J. Villain, Z. Phys. B 33 (1979) 31.
[4] H.T. Diep (Ed.), Magnetic Systems with Competing Interactions, World Scientific, Singapore, 1994.
[5] See Proceedings of Waterloo Conference on Highly Frustrated Magnetism: Can. J. Phys. 79 (2001) 1283–1596.
[6] M.J. Harris, S.T. Bramwell, D.F. McMorrow, T. Zeiske, K.W. Godfrey, Phys. Rev. Lett. 79 (1997) 2554–2557.

[7] A.P. Ramirez, A. Hayashi, R.J. Cava, R. Siddharthan, B.S. Shastry, Nature 399 (1999) 333–355.
[8] M.J. Harris, S.T. Bramwell, D.F. Mcmorrow, T. Zeiske, K.W. Godfrey, Phys. Rev. Lett. 79 (1997) 2554–2557.
[9] R. Siddharthan, et al., Phys. Rev. Lett. 83 (1999) 1854–1857.
[10] J. Snyder, J.S. Slusky, R.J. Cava, P. Schiffer, Nature 413 (2001) 48–51.
[11] J. Snyder, et al., Phys. Rev. B 69 (2004) 064414.
[12] D. Davidovic, et al., Phys. Rev. Lett. 76 (1996) 815–818.
[13] H. Hilgenkamp, et al., Nature 422 (2003) 50–53.
[14] R.P. Cowburn, M.E. Welland, Science 287 (2000) 1466–1468.
[15] C.A. Ross, et al., J. Appl. Phys. 91 (2002) 6848–6853.
[16] R.P. Cowburn, Phys. Rev. B 65 (2002) 092409.
[17] J.I. Martin, J. Nogues, K. Liu, J.L. Vicent, I.K. Schuller, J. Magn. Magn. Mater. 256 (2003) 449–501.
[18] A. Imrea, G. Csabaa, G.H. Bernstein, W. Porod, V. Metlusko, Microstruct 34 (2003) 513–518.
[19] R.L. Stamps, R.E. Camley, J. Magn. Magn. Mater. 177 (1998) 813–814.
[20] R.F. Wang, et al., Nature 439 (2006) 303–306.
[21] S.T. Bramwell, Nature 439 (2006) 273–274.
[22] P. Politi, M.G. Pini, Phys. Rev. B 66 (2002) 214414.
[23] G.T. Barkema, M.E.J. Newmann, Phys. Rev. E 57 (1998) 1155.
[24] M.E.J. Newmann, G.T. Barkema, Clarendon Press, Oxford, 1999.
[25] L.M. Schmitt, S. Droste, in: Proceedings of the 8th Annual Conference on Genetic and Evolutionary Computation, 2006, pp. 879–886, ISBN:1-59593-186-4.
[26] L.M. Schmitt, Asymptotic convergence of scaled genetic algorithms to global optima—a gentle introduction to the theory, in: A. Menon (Ed.), Frontiers of Evolutionary Computation, Kluwer, Dordrecht, The Netherlands, 2004, pp. 157–192.
[27] P. Sutton, D. Hunter, N. Jan, J. Phys. I France 4 (1994) 1281.